

# Relative Positioning using RTK Measurement Filtering and PPP

G. Seepersad, J. Aggrey, M. Gill, and S. Bisnath, *York University*  
D. Kim and H. Tang, *Gemini Navsoft Technologies Inc.*

## BIOGRAPHIES

Garrett Seepersad is a Ph.D. candidate at York University, Toronto, Canada, in the Department of Earth and Space Science and Engineering. He has completed his honours B.Sc. in Geomatics at the University of West Indies and his M.Sc. in Geomatics Engineering at York University. His area of research currently focuses on the development and testing of PPP functional, stochastic and error mitigation models.

John Aggrey is a Ph.D. candidate at York University, Toronto, Canada, in the Department of Earth and Space Science and Engineering. He has completed his B.Sc. in Geomatics at the Kwame Nkrumah University of Science and Technology. His area of research currently focuses on the development and testing of GNSS PPP software development, and PPP functional, stochastic and error mitigation models.

Maninder Gill is a M.Sc. candidate at York University, Toronto, Canada, in the Department of Earth and Space Science and Engineering where he also completed his B.Eng. in Geomatics Engineering. His area of research currently focuses on the development of low cost GNSS PPP technology.

Dr. Sunil Bisnath is an Associate Professor in the Department of Earth and Space Science and Engineering at York University in Toronto, Canada. His research interests include geodesy and precise GNSS positioning and navigation.

Dr. Don Kim is an adjunct professor in the Department of Geodesy and Geomatics Engineering at the University of New Brunswick and the CEO at Gemini Navsoft Technologies Inc. His research interests include high-precision positioning and navigation for deformation monitoring and machine auto-steering. He shared the Dr. Samuel M. Burka Award for 2003 from The Institute of Navigation with Dr. Richard B. Langley.

Dr. Hui Tang is a Research Engineer at Gemini Navsoft Technologies Inc. She received her Ph.D. from the University of New Brunswick in 2014. Her research focus is signal spectrum analysis and measurement band-pass filtering for high-precision positioning applications. She

also has interest in high-precision, indoor positioning and navigation using multi-sensor integration.

## ABSTRACT

Typical RTK performance is limited to baselines of <10-15 km, as longer distances cause increased measurement errors, which cannot be successfully managed by processing software. The objective of relative positioning is to reduce or eliminate error sources by mathematically differencing simultaneous GNSS measurements from multiple receivers. Accuracy is correlated with baseline length and amounts to approximately 0.1 to 1 ppm for baselines up to some 100 km and then less for longer baselines. The great benefit of PPP is that this technique relies on only single receiver point positioning combined with precise satellite orbit and clock information, code and phase observable filtering, and additional error modelling. PPP is limited by the need for tens of minutes of measurements in order for dm-level positioning, and hours of measurements for cm- and mm-level positioning.

Compared to conventional RTK, the RTK measurement filtering approach not only simplifies the implementation of data processing algorithms, but also avoids the risks induced by the commonality assumption. As the measurement filtering approach does not rely on common (correlated) error sources between satellites and receivers, as is the case with conventional RTK, it is immune to long baseline conditions as well as localized anomalous atmospheric conditions. Unlike the PPP approaches, this filtering approach requires neither sophisticated error modelling nor high quality products from international geodetic science organizations (e.g., IGS precise orbit and clock products), as most of the significant error sources can be filtered out using an appropriate signal filter.

Although PPP and RTK techniques are now being used as inter-changeable approaches, both have their advantages with regards to long baseline relative positioning. Presented in this paper are novel approaches using RTK with filtered measurements that reduces noise, and inadvertently, eliminates associated errors. The approach saw significant improvement over the traditional RTK technique from the metre level to sub-decimeter level. The PPP approach was used as a comparison tool to ascertain how long a baseline or large a height difference can be

processed by the RTK technique, before PPP would become a reliable alternative.

## INTRODUCTION

There is a growing demand from GNSS end users for accurate positioning techniques and services. RTK, the industry and scientific standard, and now PPP, are utilized in a variety of different commercial applications such as crustal deformation monitoring and precise positioning of mobile objects. The main commercial applications are found in the agricultural industry for precision farming, marine applications for sensor positioning in support of seafloor mapping and marine construction, and airborne mapping, for photogrammetric sensor positioning.

The objective of this paper is to study the benefits and limitations of each technique for high-precision relative positioning applications. Outcomes include a unique study of PPP relative positioning performance, the use of novel measurement filtering in relative positioning and a comprehensive comparison of the utility of each technique.

Conventional RTK performance is limited to baselines of less than 15 km, as longer baselines cannot effectively account for measurement errors. The objective of relative positioning is to reduce or eliminate error sources by mathematically differencing simultaneous GNSS measurements from multiple receivers. Accuracy is correlated with baseline length and amounts to approximately 0.1 to 1 ppm for baselines up to some 100 km and then less for longer baselines (Euler and Schaffrin, 1991). The benefit of PPP is that it removes the requirement of a local GNSS network allowing millimetre to centimetre level positioning accuracy with a single GNSS receiver. PPP is limited by the need for tens of minutes of measurements in order for dm-level positioning, and hours of measurements for cm- and mm-level positioning.

Since GNSS range measurements contain a variety of error components in the frequency spectrum, measurement filtering can effectively remove error components with well-characterized frequencies. In contrast to conventional RTK, a measurement filtering approach not only simplifies the implementation of data processing algorithms, but also avoids the risks induced by the commonality assumption (a single set of shared assumptions or properties between the reference and rover stations). As the measurement filtering approach does not rely on common correlated error sources between satellites and receivers, unlike conventional RTK, it is immune to long baseline conditions (less than 75 km) as well as localized irregular atmospheric conditions. Unlike the state space corrections applied in PPP, measurement filtering requires neither sophisticated error modelling nor high quality products such as precise orbit

and clock products, as most of the significant error sources can be filtered using an appropriate signal filter.

Single point positioning techniques are calculated relative to a well-defined global reference system, in contrast to relative positioning, where the coordinates are in relation to a fixed reference point. The accuracy of static relative positioning with a geodetic-grade receiver has been typically 5 mm + 0.5 ppm (rms) for the horizontal component and 5 mm + 1 ppm (rms) for the vertical component (Eckl et al., 2001) representing the highest accuracy possible which deteriorates exponentially as the length of the baseline increases.

In order to determine if it is possible to replace post-processed, static, relative positioning with RTK and PPP, data from varying baseline length are analyzed. Initial RTK processing was performed with the Gemini Navsoft Technologies Inc. mmVu measurement filtering engine, and PPP processing with the York-PPP engine.

## RTK MEASUREMENT FILTERING APPROACH

The generic GNSS signal tracking corresponds to receiving a signal propagated through transmission media over a noisy channel. The received signal contains a known deterministic signal (i.e., the range between a satellite and a receiver) mixed with a coloured noise.

If the process associated with the GNSS observations is white, estimation problems are relatively easy to formulate, solve and analyze. When the process is coloured rather than white, the easier results from the white case can still often be invoked in some appropriate way if the coloured process is transformable into a white process by passing it through a whitening filter, which flattens out the spectral characteristics of the coloured process presented at the input into those of the white noise obtained at the output.

The conceptual diagram of the measurement filtering approach is illustrated in Figure 1, where  $\Phi_t$  represents the GNSS observation comprising of the range  $\rho_t$  and a coloured noise  $v_t$ .

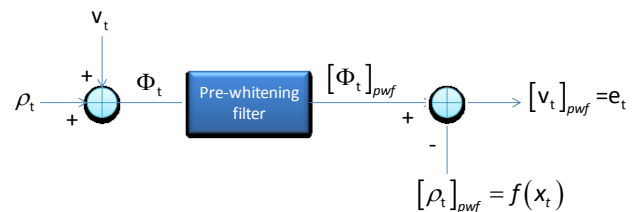


**Figure 1: Measurement Filtering approach for position estimation**

Assuming that a whitening filter can be designed appropriately for GNSS data processing, the filtered observation is expressed as:

$$[\Phi_t]_{pwf} = [\rho_t]_{pwf} + [v_t]_{pwf} = f(x_t) + e_t, \quad (1)$$

where  $[ ]_{pwf}$  is a whitening process,  $f(x_t)$  is the functional model of the filtered range which can be formulated with the receiver position  $x_t$  to be estimated, and  $e_t$  is the filtered noise (e.g., ideally a white noise). Equation (1) implies two fundamental conditions associated with the Measurement Filtering approach as:

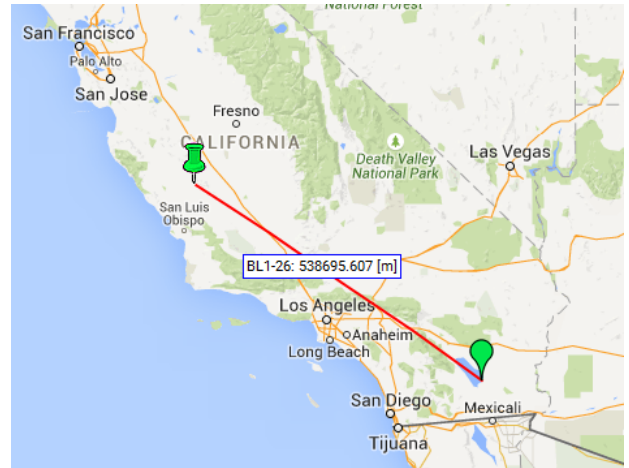
- 1) The filtered range obtained through a whitening process should be a function of the receiver position to be estimated.
- 2) The spectral characteristics of the filtered noise are required to be white.

The conventional RTK approach whitens (conceptually) the observations by removing common error sources at both satellites and receivers. Typically double-difference (DD) operation (that is, differencing the measurements between receivers followed by differencing between satellites or vice versa) is used to remove common effects and thus it acts as a whitening filter in the relative positioning. On the other hand, the PPP approach whitens (conceptually) the observations by utilizing precise orbit and clock information, and sophisticated error modelling algorithms.

The measurement filtering approach whitens the observations by signal filters (e.g., low-, high- and band-pass filters) (Kim et al., 2013; Kim and Griffith, 2014). Theoretically, this approach can be applied for both relative and absolute positioning techniques. Depending on the positioning technique applied for GNSS data processing, input observations and filter design will be different to some degree.

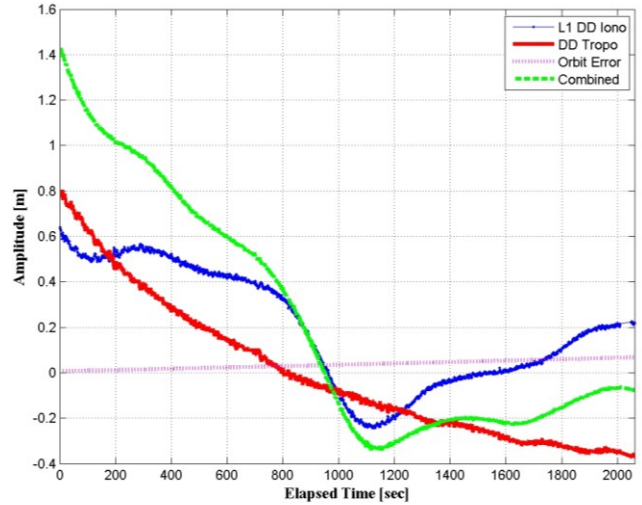
To give more insights of the measurement filtering approach, an example case of long-baseline, relative positioning (see Figure 2) is explained hereafter. Instead of the details of filter formulation, illustrations are used for simplification.

Considering relative positioning does not rely on external precise orbit and clock information, the most significant error sources are satellite orbit and clock error, atmospheric delay and multipath. It would not be difficult to evaluate the power of individual error source (or a compound of error sources) in the error spectrum that we could design an efficient and effective filter for high precision GPS data processing.



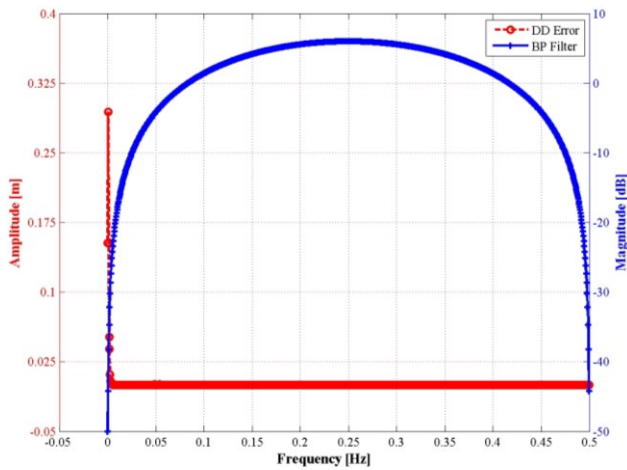
**Figure 2: A sample baseline on the SOPAC network (stations POMM and P507, about 540 km baseline, GPS only observation at a 1 Hz data rate)**

Figure 3 illustrates typical GPS error sources in the long-baseline observations. DD ionospheric delay on the L1 carrier phase (L1 DD Iono) was roughly estimated using the geometry-free linear combination of L1 and L2 observations. IGS precise orbit information and the ionosphere-free linear combination of L1 and L2 observations were used to estimate DD tropospheric delay (DD Tropo). DD range error due to Broadcast Ephemeris (Orbit Error) was estimated using IGS precise orbit information.



**Figure 3: GPS error sources in the DD carrier phase observations (PRN14 and PRN22)**

The frequency response of the GPS error sources (combined) and a band-pass filter is illustrated in Figure 4 and Figure 5.



**Figure 4: Frequency response of the DD error sources (DD Error) and a band-pass filter (BP Filter)**

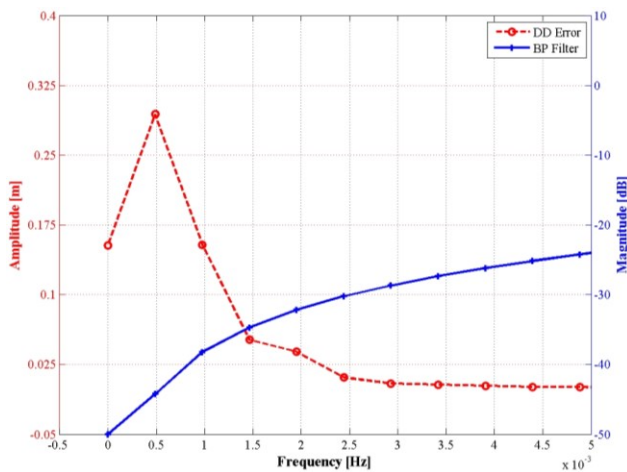


**Figure 5: Frequency response of the DD error sources and a band-pass filter (the low-frequency part of Figure 4)**

As it turns out, most of significant GPS error sources are dominant in low-frequency (e.g., below 0.0014 Hz or over a 700-second cycle) and a band-pass filter can effectively attenuate the low-frequency error components more than 100 times (i.e., below -40 dB).

Figure 6 shows the filtered GPS observations and errors through a band-pass filter. GPS L1 DD carrier phase observations for PRN14 and PRN22 were used. The top panel presents filtered DD ranges, while the bottom panel shows filtered DD errors.

Note that the filtered range (the top panel in Figure 6) should be expressed as a function of the receiver position to be estimated as explained in Equation (1). In general, to improve the spectral characteristics of the filtered errors, a different input observation and filter design can be used depending on applications (Tang and Kim, 2014).

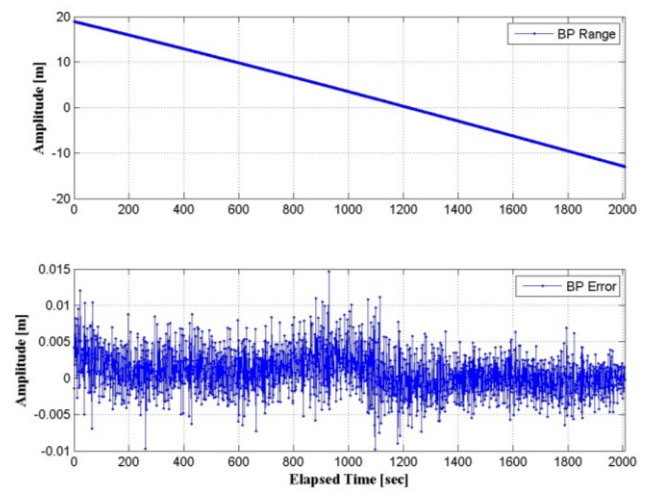


**Figure 6: Filtered observations and errors**

The measurement filtering approach utilized within this analysis uses relative baseline processing, L1 GPS carrier phase observations, broadcast ephemeris and GNT's proprietary Time Delayed Doppler (TTD) and Double Differenced Carrier (DDC). The TDD filter is a band pass filter that can mitigate error sources and noise of GNSS observations having low- and high-frequency components within the error spectrum. The TDD works well under more challenging conditions such as long baselines (> 30 km) and significant height difference (> 500 m).

## PPP BASELINE PROCESSING

The PPP utility from York University (YorkU-PPP) was built in 2012. It is capable of processing GPS observations in real-time (Seepersad, 2012) and has been expanded to process observations from multi-GNSS constellations (Aggrey, 2015). Other GNSSs are currently being established which includes Galileo and BeiDou. YorkU-PPP is capable of producing sub-centimetre accuracy in the horizontal component and centimetre in the vertical. Multi-GNSS data from 350 IGS stations observed during DOY 195 to 201 in 2014 were processed using the YorkU-PPP software. PPP solutions in the horizontal and vertical components had rms of 1 and 2 mm, respectively (Aggrey 2015). A more detailed description of the YorkU-PPP software architecture can be found in (Seepersad, 2012; Aggrey, 2014).

PPP is a standalone approach to GNSS positioning that is not restricted by a regional network distribution or requirement of a localized GNSS reference receiver. The independence of PPP is an important advantage for point positioning and calculating baseline lengths over RTK technique, as errors with RTK positioning are mostly localized. Bertiger et al. (2010) and Seepersad and Bisnath (2014) illustrated that PPP is capable of producing baseline lengths of few millimetres accuracy for baselines less than 1000 km and the accuracy for baselines between 1000 to

10,000 km decreased to sub-centimetre accuracy (Bertiger et al. 2010). To calculate the baselines between the reference and rover stations, the following equation was used

$$d_{3D} = \sqrt{(dN_{B-R} + \sigma N_{B-R})^2 + (dE_{B-R} + \sigma E_{B-R})^2 + (dU_{B-R} + \sigma U_{B-R})^2} \quad (1)$$

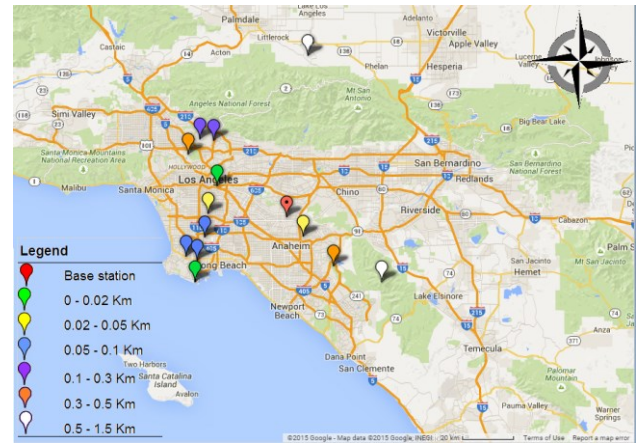
where  $d^*_{B-R} = d^*_B - d^*_R$ , such that \* represents either northing, easting or up component and  $B$  is the base/reference station and  $R$  is the rover station.

## DATASET AND PROCESSING PARAMETERS

To determine if it is possible to replace post-processed static relative positioning with RTK and PPP, one month of 1 Hz GPS measurements from 21 baselines ranging from 20 to 300 km in Southern California from January 2015 were processed. Southern California was selected because of its mixed terrain type and high density of reference stations. RTK processing was performed with the Gemini Navsoft Technologies Inc. mmVu measurement filtering engine, mmVu LabSync and PPP processing with the York-PPP engine. Processed results were compared against the reference solutions provided by Scripps Coordinate Tool (Scripps, 2015).

The YorkU-PPP processing parameters used was static mode for the reference stations coordinates. Receiver clocks were estimated epoch-by-epoch. The zenith tropospheric delays were also estimated each epoch with a random walk co-efficient of 2 cm/sqrt(hour). The station coordinates were initialized using a pseudorange only solution with an initial constraint of 10 m. The IGS absolute antenna model file was used and ocean loading coefficients were obtained from Scherneck (2013) for each of the sites processed. Within mmVu LabSync, time delayed Doppler filter (TDD) was used for processing and uncertainty value of 0.005 mm (Q) was added to the covariance matrix. The smaller the value of uncertainty (Q) translates to the smaller uncertainty in the unknowns. On the other hand larger uncertainty allows the filter to respond more quickly, but results in greater uncertainty in the unknowns.

Results were grouped in two processing scenarios, varying altitude differences and varying baselines lengths. These scenarios were chosen because they are the dominant physical factors that affect the accuracy of RTK. The geographic distribution of the 13 GNSS stations with varying altitude differences ranging from 0.02 to 1.6 km is presented in Figure 7.



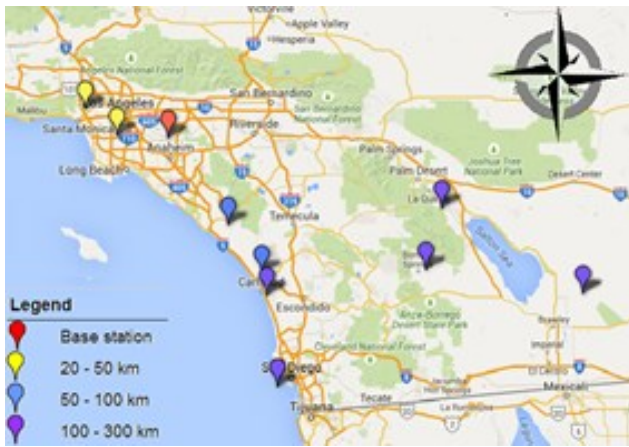
**Figure 7** Distribution of selected GNSS stations with varying altitude differences ranging from 0.02 to 1.6 km with a maximum baseline length of less of 59 km

Table 1 presents an overview of the different stations selected to analyze the solution performance for varying altitude differences, the baseline length of for each station and if the data consisted of GPS-only or GPS and GLONASS.

Altitude (km)	Station	Baseline	GNSS processed
0-0.02	vtis	41	G
	elsc	28	G
0.02-0.05	mhms	29	G
	cccs	9	G + R
0.05-0.1	csdh	31	G
	hbco	36	G
	torp	40	G + R
0.1-0.3	bran	43	G
	vdcy	39	G + R
0.3-0.5	leep	43	G
	oeoc	25	G + R
0.5-1.6	hol3	59	G
	mjpk	42	G + R

**Table 1:** GNSS stations selected with varying altitude differences ranging from 0.02 to 1.6 km with a baseline length of less than 60 km. G represents GPS only and G+R represents GPS and GLONASS. All units are in kilometres.

Presented in Figure 8 is the geographic distribution of the 9 GNSS stations with varying baselines ranging from 20 to 300 km with a maximum altitude difference of 0.091 km.



**Figure 8: Distribution of selected GNSS stations selected with varying baselines ranging from 20 to 300 km with a maximum altitude difference of 0.091 km**

Table 2 presents an overview of the different stations selected to analyze the solution performance based on different baseline lengths. 9 GNSS stations were selected, with a maximum altitude difference of 91 m. Due to the altitude restriction, no stations with GPS and GLONASS was available for processing.

Baseline (km)	Station	Altitude (m)	GNSS processed
20-50	uclp	0.045	GPS
	mhms	0.069	
50-100	rmvj	0.070	
	ocsd	0.024	
100-300	clbd	0.046	
	p475	0.091	
	p491	0.062	
	p486	0.060	
	p510	0.065	

**Table 2: GNSS stations selected with varying baselines ranging from 20 to 300 km with a maximum altitude difference of 0.091 km. All units are in kilometres.**

### ANALYSIS OF RTK AND PPP SOLUTION PERFORMANCE

To examine the benefits and limitation of RTK and PPP, datasets were examined under varying conditions. These included, varying baselines, which ranged from 20 to 300 km, varying altitude differences, which ranged from 0.2 to 1.6 km and solution stability.

#### Typical solution quality of PPP and RTK

Shown in Figures 9 and 10 are the positioning results for both PPP and RTK techniques, respectively. The results are obtained from a static dataset from WHC1 which is part of the Southern California network. Figure 10 however shows

the 20km baseline RTK results between WHC1 and CSDH.

The PPP results show how the coordinate estimates slowly converge to centimetre level with 20 – 30 minutes. However, RTK typically achieves an instantaneous convergence within a few seconds. Given in Tables 3 and 4 are the positioning accuracy statistics for both PPP and RTK, respectively.

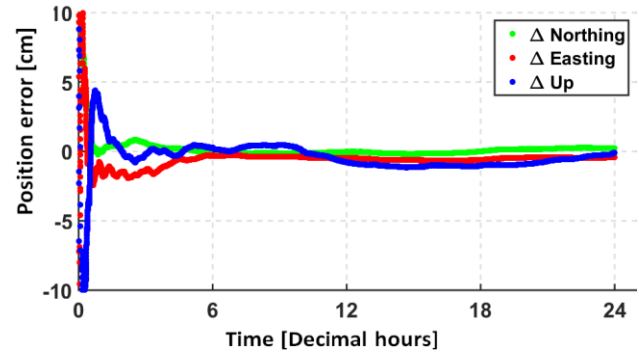


**Figure 9: 3D difference in position error for WHC1 24 hour dataset for DOY 29 in 2015. Result was obtained in static processing mode.**

	2D	Up	3D
Bias	0.5	0.1	0.5
Std dev	0.1	0.3	0.3
rms	0.5	0.3	0.5

**Table 3: 2D, 3D and Up component statistics for station WHC1 24 hour dataset for DOY 29, processed in static mode. All units are in centimetres.**

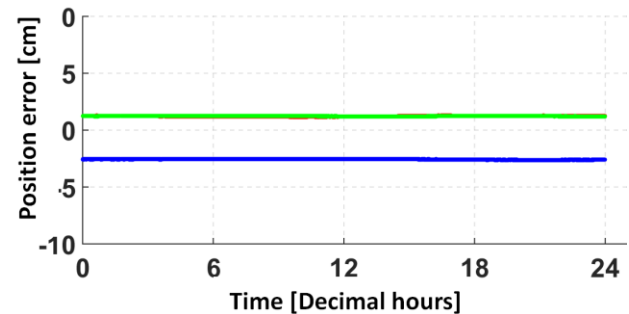


**Figure 10: 3D difference in position error for stations WHC1 and CSDH 20km baseline for DOY 29 in 2015. Result was obtained in static processing mode.**

	2D	Up	3D
Bias	1.7	-2.8	3.1
Std dev	0.02	0.01	0.04
rms	17	27	31

**Table 4: 2D, 3D and Up component statistics for stations WHC1 and CSDH 20km baseline for DOY 29, processed in static mode. All units are in centimetres.**

It must be noted that there is a significant bias in the Up component for RTK, as compared to PPP. Atmospheric conditions typically affects the RTK processing with a metre level magnitude of error, especially as the baseline length increases. However, RTK shows a higher precision than RTK as shown in their respective standard deviations

### Solution quality based on varying baseline length

A major limitation of traditional RTK is that in order to achieve a high level of precision, the rover station has to be within a few kilometres proximity of the reference station. With typical RTK positioning, the ionosphere and troposphere introduces systematic errors which limits the allowable baseline length to about 20 km if reliable user solutions are required (Tobias et al., 2011). As the baselines increases, the accuracy of the solutions decreases and this decrease becomes noticeable in the metre level of errors.

The baselines ranged from 20 to 300 km to examine the position quality from mmVu LabSync and YorkU-PPP. The altitude differences were restricted to a maximum difference of 91 m to prevent unmodelled errors due to relative positioning. Stations were divided into three intervals based on the baseline length, ranging from 20 to 50 km, 50 - 100 km and 100 - 300 km. Baseline ranging from 20 to 50 km were used as a control to examine solution performance that experience relatively similar atmospheric conditions but in a more challenging environment than what is expected by conventional RTK. As the baseline lengths increased, filtering performance was analyzed to examine performance in more challenging environments.

Table 5 shows the varying baselines between these stations and the reference stations. The stations, as presented in the table, are plotted in a consecutive order in Figure 11 for both PPP and RTK. Stations OCS D, CLBD, P510 and P475 have baselines that range from 20 to 300 km. For RTK, as the baseline increases, the errors are de-localized and the solution quality deteriorates, especially in the Up and 3D components, even though the altitude remains relatively constant.

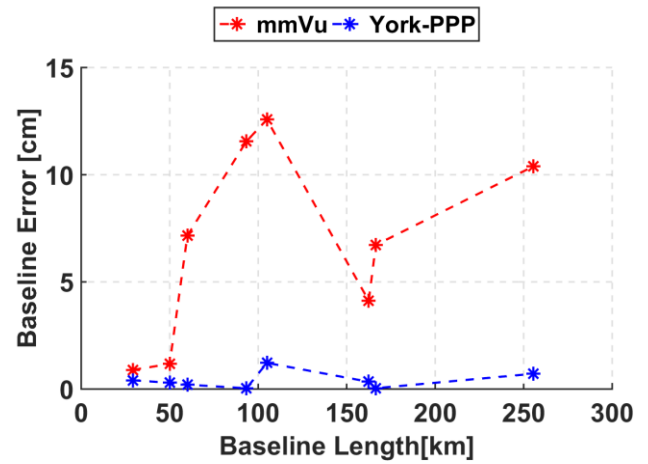


**Figure 11: Baseline error of GNSS stations with constant altitude (less than 100 m) and varying baseline lengths processed by mmVu LabSync and York PPP**

Length (km)	Station	mmVu		PPP	
		$\Delta 2D$ (cm)	$\Delta Up$ (cm)	$\Delta 2D$ (cm)	$\Delta Up$ (cm)
20-50	mhms	0.7	10.0	0.4	1.6
	uclp	1.6	0.3	0.4	0.9
50-100	rmvj	8.4	26.0	1.9	3.7
	ocsd	0.1	16.5	0.7	1.8
100-300	clbd	1.5	12.2	0.4	2.0
	p491	2.1	16.9	0.6	2.4
	p486	0.2	24.1	0.1	0.6
	p510	4.4	29.1	0.8	0.4

**Table 5: Summary statistics for each station and position component for the GNSS stations with varying baselines ranging from 20 to 300 km processed by mmVu LabSync and York PPP**

The same stations were also processed by YorkU-PPP engine to examine the solution performance. Overall, the results generated by the YorkU-PPP are consistent and stable in the centimetre to millimetre level as seen in the statistics in Table 5. Given that PPP performs irrespective of the baseline lengths, there is no unique trend noticed as observed for the RTK technique. All stations showed millimetre level of accuracy with the horizontal components and centimetre to few centimetres in the dU and d3D components. In summary, given a constant altitude of approximately 100 m, PPP becomes a reliable alternative to RTK with baselines longer than 50 km where the atmospheric errors are de-localized.

### Solution quality based on varying altitude differences

Also examined was the variability of the position estimates from RTK and PPP for varying altitude differences but a constant baseline length. Due to data availability, constant baseline in this context was any baseline less than 60 km.

Sites were grouped into six different intervals. The first interval selected was from 0 to 0.02 km to analyze the position error in an ideal environment. The bin sizes increased 20-50, 50-100,100-300, 300-100 and 500-1600 to observe the effects of increasing altitude differences.

Shown in Figure 12 are 13 stations with varying altitudes but having a constant baseline (within 60 km) for RTK and PPP. Table 6 highlights changing horizontal and vertical components with respect to the reference station. Stations OEOC, HOL3 and MJPk had error of 38, 72 and 162 cm, respectively, as the altitudes of these stations increased.

As stated beforehand, the raw pseudorange and carrier-phase measurements are filtered using a band pass filter to spectrally remove the errors without the need for estimation or modelling. However, due to a strong correlation of the height of stations with the tropospheric delay over longer baselines ( $>20$  km) (Rothacher, 2002), it is problematic to comprehensively eliminate the effect of the troposphere. Stations OEOC, HOL3 and MJPk have heights that range 300 to 500 m with baselines over 20 km.

A possible explanation for the errors seen in these stations, is potentially due to existing tropospheric effect though spectrally removed over a relatively longer baseline than the conventional distance of about 20 km.

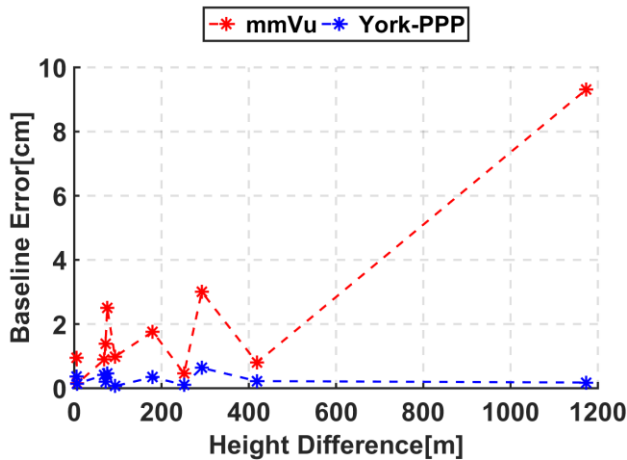


Figure 12: Baseline error of GNSS stations with constant baseline (less than 60 km) and varying height differences processed by mmVu LabSync and York PPP

Alt. (m)	Station	mmVu		PPP	
		d2D (cm)	dUp (cm)	d2D (cm)	dUp (cm)
0-20	elsc	2.7	5.6	0.2	0.8
	vtis	2.5	0.5	0.1	0.6
20-50	mhms	0.7	10.0	0.4	1.6
	torp	1.2	19.8	0.2	0.3

50-100	csdh	1.6	11.4	0.5	0.5
	hbco	0.4	10.4	0.4	2.5
	bran	4.1	12.5	0.7	0.5
100-300	vdcy	5.6	19.8	1.7	4.0
	oecoc	12.6	36.1	0.7	2.2
300-500	leep	5.9	29.3	0.2	1.5
	hol3	100.9	118.2	2.6	3.1
500-1600	mjpk	44.8	161.3	1.3	2.3

Table 6: Summary statistics for each station and position component for the GNSS stations with varying height differences ranging from 0 to 1200 m processed by mmVu LabSync and York PPP

The PPP results again performed better than the RTK results presented in Figure 12. The PPP baseline error values are stable in the millimetre level as compared to the metre level presented in the RTK solution. It is noteworthy to observe that with a constant baseline length, PPP again serves as an alternative to the RTK, when height differences reach beyond 400 m.

### RTK baseline vector rotation and scale change

It turned out RTK baseline solutions have noticeable biases in the position component as outlined in Table 5 and 6. In the relative positioning technique, a fixed base station, a known satellite orbit position and the range measurements of base and rover stations constrain the geometry of the baseline in its estimation process. As illustrated in Figure 9, errors in the satellite position and range measurements can change the geometry of the baseline and thus result in baseline vector rotation and scale change. In fact, the biases of baseline solutions are induced by the combined effects of baseline vector rotation and scale change. As mmVu's measurement filtering technique can reduce the errors in the range measurements (see the bottom panel in Figure 6), the biases of position component are mainly due to the satellite position errors. Note that broadcast ephemeris was used for RTK baseline processing in this paper.

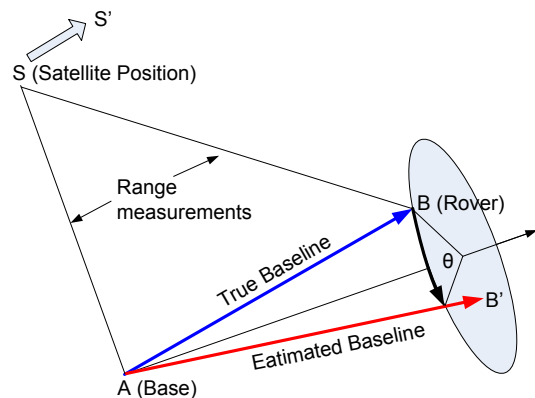
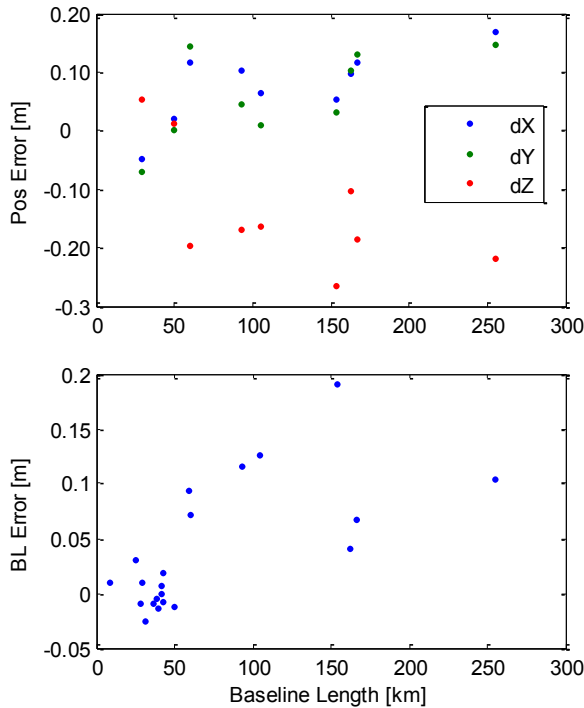


Figure 9: Baseline rotation and scale change

Compared to the biases of position component, it turned out that the baseline length error (i.e., baseline scale

change) is less sensitive to the satellite position errors. As illustrated in Figure 10, the baseline length error for the baselines up to 50 km is within a few centimetre level. Even for long baselines up to 300 km, the baseline length error is better than about one decimetre.



**Figure 10: Position component biases (top) and baseline length error (bottom)**

Generally the errors in satellite position and range measurements induce a very small baseline vector rotation which can amplify the bias of position component according to baseline length. This is the limitation of a single-baseline RTK approach under a long baseline scenario. Note that broadcast ephemeris, single-baseline RTK was our test scenario in this paper.

The baseline length error analysis suggests network adjustment (using baseline length estimates rather than baseline component estimates) can improve long baseline RTK. Overall, precise orbit might be more substantial than network adjustment for long baseline applications because satellite position error is the main source of baseline vector rotation in our approach. We will further investigate this issue in near future.

**Position stability**

To examine position stability, peak-to-peak analysis was used. The peaks were computed as the differences between the maximum and minimum coordinates of the position components (northing, easting and up) within hourly bins. Figure 13 shows the hourly peak-to-peak solution errors. The rover stations, with reference to the base station, are of

varying baselines and altitudes. The peak-to-peak analysis presented is at the millimetre level for any hour of a 24 hour period. Shown in Figure 13 is the histogram of the peak ranges on an hourly basis for the horizontal and up components. The peak solution errors show stability in the RTK technique given the consistent precision of the solutions as 95% and 92% of the stations had an error of 1 mm in the horizontal and vertical components, respectively. For deformation monitoring purposes, the stability of the solutions over any time period is significant in obtaining high solution quality. The 1<sup>st</sup> and 24<sup>th</sup> hours showed a higher variation in the solution errors possibly due to the lower elevation of the satellites with significant orbital errors. As the day progress from the 1<sup>st</sup> to the 18<sup>th</sup> hour, the solution gets better possibly due to more measurements being processed.

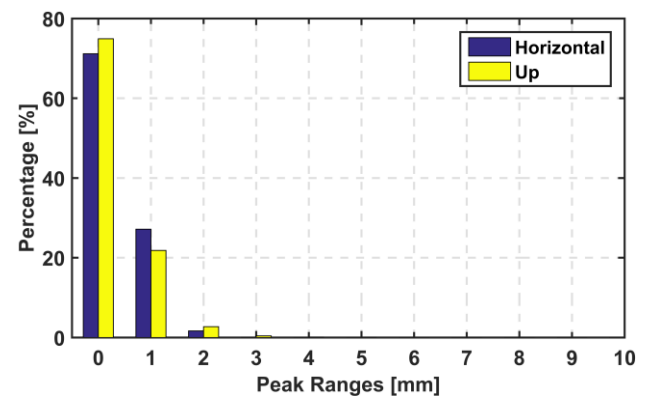


**Figure 11: Peak-to-peak histogram analysis of stations. Data was processed by mmVu LabSync .**

The hourly peak-to-peak solution errors for PPP are shown in Figure 14. Unlike RTK where float ambiguities quickly converge to integers, PPP typically requires tens of minutes in the first hour to fix ambiguities. As shown in the histogram, 83% and 70% of the stations had an error of 1 mm in the horizontal and vertical components, respectively. Compared to RTK, the instability of the peak ranges in PPP is possibly due to slow convergence of the PPP solution to the decimetre level of accuracy. However, the peak ranges improved to centimetre to millimetre accuracy for the rest of the 24 hour period. By hour 24, the peak ranges were at the millimetre-sub-millimetre level. In contrast to PPP, the RTK peak ranges were stable within each hour at the millimetre level. For deformation monitoring purposes, the consistency in the stability of the mmVu peak ranges prove to be a valuable attribute.

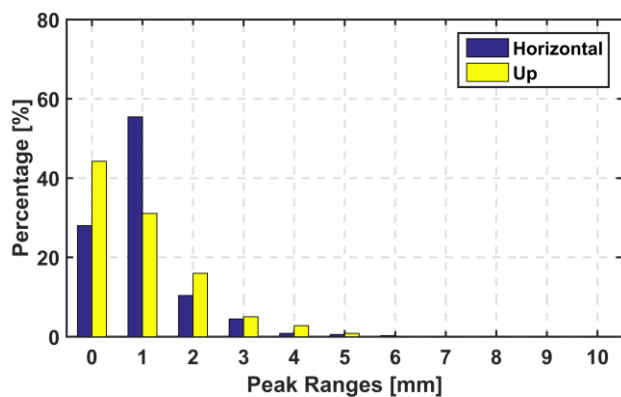


**Figure 12: Peak-to-peak histogram analysis of stations. Data was processed by YorkU-PPP.**

## CONCLUSIONS AND RECOMMENDATIONS

Conventional RTK technique over short baselines relies on the differencing of GNSS measurements to eliminate systematic errors. Presented, was an alternative approach of eliminating the errors in the raw measurements spectrally through a low band pass filter. Measurement filtering eliminates the need for the mathematical modelling or estimation of the errors. The measurement filtering approach in relative positioning was compared to PPP in long baseline processing.

The results from mmVu showed a greater stability at the millimetre level as compared to PPP peak to peak analysis. The level of stability illustrated meant that PPP, after convergence and mmVu can be utilized for applications such as deformation monitoring. Even though PPP performed better than mmVu over long baselines, the level of stability of the solutions was at the decimetre level. Given that PPP is a standalone approach that depends on the precision of satellite orbits and clocks, as well as atmospheric errors being modelled or eliminated, it was expected that over longer baselines, there would be no significant change in the solution quality irrespective of the height of a station or the length of a baseline. In summary, PPP was seen to be a reliable alternative to RTK when baseline lengths and heights exceeded 50 km and 400 m, respectively.

Intended future work would include improving the spectral detection of systematic errors of the raw GNSS measurements. All the results presented were static solutions. Future work would look at the kinematic approach, as well real-time processing of the measurements.

## ACKNOWLEDGMENTS

This research was funded by the Natural Sciences and Engineering Research Council of Canada. The results

presented are derived from data and products provided by, Scripps Institution of Oceanography and the International GNSS Service.

## REFERENCES

Aggrey J (2014). *Multi-GNSS Precise Point Positioning Software Architecture and Analysis of GLONASS pseudorange biases*. York University, Toronto, Canada, pp. 46-83.

Bisnath S and Y Gao (2009). *Current State of Precise Point Positioning and Future Prospects and Limitations*. International Association of Geodesy Symposia – "Observing our Changing Earth", 133, pp. 615-623.

Bertiger W, Desai SD, Haines B, et al (2010) Single receiver phase ambiguity resolution with GPS data. *J Geod* 84:327–337. doi: 10.1007/s00190-010-0371-9

Eckl, M.C., R. Snay, T. Soler, M.W. Cline, and G.L. Mader (2001) *Accuracy of GPS derived relative positions as a function of interstation distance and observing session duration*, *Journal of Geodesy*, Vol. 75, pp. 633-640.

Euler H-J, Schaffrin B (1991) *On a measure for the discernibility between different ambiguity solutions in the static-kinematic GPS-mode*. In: *Kinematic Systems in Geodesy, Surveying, and Remote Sensing*. Springer, pp 285–295.

Kim, D., C. Griffith, B. Haagensen, S. H. Park, D. J. Cho and K. Y. Seo (2013). *Performance evaluation of precise point positioning and long-range baseline approach used in offshore applications*. Presentation viewgraph, GNSS PPP Workshop: Reaching Full Potential, Ottawa, Canada, June 12-14.

Kim, D. and C. Griffith (2014). *Effects of tropospheric delays in mm-level high-precision GNSS deformation monitoring*. *Journal of Korean GNSS Society* (submitted).

Rothacher, M (2002) *Estimation of Station Heights with GPS*. International Association of Geodesy Symposia Volume 124, 2002, pp 81-90

Scripps (2015) *SECTOR GPS Site Coordinate Estimator*. <http://sopac.ucsd.edu/sector.shtml>. Accessed 24 Jun 2015

Scherneck H (2013) *Ocean Tide Loading Provider*. <http://froste.oso.chalmers.se/loading/index.html>. Accessed 2 Jan 2013

Seepersad, G. (2012) *Reduction of initial convergence period in GPS PPP data processing*, MSc thesis, York University, Canada, pp. 1-131.

Seepersad G, Bisnath S (2014) *Challenges in Assessing PPP Performance*. Journal of Applied Geodesy 8:205–222.

Tang, H. and D. Kim (2014). *Design of a band-pass filter for monitoring structural vibration due to earthquake using GNSS*. GNT Technical Report for Obayashi Corporation.

Tobias, Guillermo, Garcia, Cristina, Mozo, Alvaro, Navarro, Pedro, Piriz, Ricardo, Rodriguez, Irma, Rodriguez, Daniel, *Filling in the gaps of RTK with Regional PPP*, Proceedings of the 24th International Technical Meeting of The Satellite Division of the Institute of Navigation (ION GNSS 2011), Portland, OR, September 2011, pp. 2193-2201.